Investigation of structural and chemical ordering in Si-rich amorphous SiC alloys via Raman spectroscopy and numerical modelling

2001 J. Phys.: Condens. Matter 13 10743

(http://iopscience.iop.org/0953-8984/13/48/301)

INSTITUTE OF PHYSICS PUBLISHING JOURNAL OF PHYSICS: CONDENSED MATTER

J. Phys.: Condens. Matter **13** (2001) 10743–10755 PII: S0953-8984(01)25925-6

Investigation of structural and chemical ordering in Si-rich amorphous SiC alloys via Raman spectroscopy and numerical modelling

A Chehaidar[1], **A Zwick**[2] **and R Carles**[2]

[1] Groupe de Physique Théorique, Département de Physique, Faculté des Sciences de Sfax, BP 802, 3018 Sfax, Tunisia

[2] Laboratoire de Physique des Solides (UMR 5477, Associé au CNRS), Université Paul-Sabatier, 118 route de Narbonne, 31062 Toulouse Cédex, France

Received 19 June 2001, in final form 13 September 2001
Published 16 November 2001
Online at stacks.iop.org/JPhysCM/13/10743

Abstract

Short-range structural and chemical ordering in Si-rich chemically deposited a-$Si_{1-x}C_x$ thin films have been investigated via Raman scattering and the numerical modelling technique. Raman spectra have been presented over a wide frequency range including both Stokes and anti-Stokes scattering. The interpretation of the spectra is performed in terms of the whole density of vibrational states. In order to determine the latter, the structure of the a-$Si_{1-x}C_x$ ($x < 0.5$) system has been modelled and the corresponding dynamical properties have been computed in the harmonic approximation using the valence-force-field model. By integrating the Stokes and anti-Stokes, first-order, and multiple-order processes, a fit of the experimental Raman spectra has been achieved. As expected, our analysis shows a tendency to chemical ordering into a tetrahedrally coordinated network for Si-rich alloys. Nevertheless, a total chemical ordering is not achieved since homonuclear C–C bonds coexist with Si–Si and Si–C ones in these alloy compounds.

1. Introduction

Amorphous silicon–carbon alloy is an attractive material from the fundamental and technological points of view. The fundamental interest lies in the modification of the chemical ordering, types of bond, and coordination between the different atomic species, with respect to the corresponding crystals. The technological interest arises from the fact that the a-$Si_{1-x}C_x$ system is one of the most important materials used as a structural ceramic, i.e. a matrix of protective coating, for thermostructural fibrous composite materials. Furthermore, its electronic and optical properties make it potentially useful in the technology of solar cells, photovoltaic devices, and refractory materials. In order to control the desired properties of

such highly disordered systems, it is of prime importance to understand the relationship of local structure and chemical arrangements to the desired physical properties.

In recent years, great effort has been devoted to the study of a-$Si_{1-x}C_x$ alloys. Among the large variety of characterization techniques, Raman spectroscopy has been particularly widely used. Nevertheless, the link between recorded spectra and atomic structure is not straightforward, since the lack of translational invariance leads to the activation of all acoustic and optical vibrational modes: the Raman spectrum will effectively look like the density of vibrational states (DVS), instead of well defined structures as for crystalline phases. Consequently, the knowledge of the DVS of amorphous compounds is of prime importance for a better interpretation of the Raman scattering in these materials.

In our previous work [1] an attempt was made to interpret the Raman scattering in hydrogenated a-$Si_{1-x}C_x$ thin films with alloy compositions $x = 0, 0.25, 0.5$ and 1. The interpretation was based on the lineshape analysis of the spectra: Raman spectra have been calculated in the framework of Zwick and Carles's model [2] by integrating first-order and multiple-order Raman processes. Nevertheless, since the DVS of the non-stoichiometric a-$Si_{1-x}C_x$ system was not available, the calculations were limited to a-Si, stoichiometric a-SiC, and a-C, using the convoluted version of the DVS of the corresponding crystalline phases. So, a careful examination of Raman scattering in non-stoichiometric a-$Si_{1-x}C_x$ alloys is necessary and modelling of the dynamical properties of these materials is fruitful for their better interpretation.

This paper is devoted to a detailed investigation of Raman scattering in Si-rich a-$Si_{1-x}C_x$ alloys. We present first the experimental spectra recorded over a wide spectral range including both Stokes and anti-Stokes regimes. We proceed then to a careful interpretation of these data. For this, the structure of a-$Si_{1-x}C_x$ alloy is modelled, and the corresponding DVS as well as the Raman spectra are computed numerically. Finally, a comparison between calculated and experimental spectra is presented, from which conclusions about the structural and chemical ordering in Si-rich alloys are drawn.

2. Experimental details

Raman spectra have been measured at room temperature from thin layers of Si-rich a-$Si_{1-x}C_x$ alloys deposited at low temperature on a crystalline SiC substrate by the CVD technique [3]. The excitation has been performed using the 488 nm line of an argon laser. The incident beam was focused using grazing incidence to limit local heating of the samples. These latter were kept under vacuum. The scattered light was dispersed through a triple monochromator, T800 Coderg, and detected by a low-noise photocounting system.

The spectra were recorded over a wide frequency range (-600–2000 cm^{-1}). By performing this unusual procedure we obtained information on both Stokes and anti-Stokes scattering and on multiple-order processes. Only the frequency-independent dark noise of the photomultiplier has been systematically subtracted from the recorded signal.

3. Calculation details

The modelling of the dynamical properties of amorphous material generally requires, on one hand, an appropriate structural model, and, on the other hand, an adequate energetic model. In an amorphous solid, the presence of chemical bonding imposes some constraints on the spatial arrangement of the atoms. The non-metallic compounds which are of interest in the present work, having mainly directed covalent bonds, can often be described by a continuous-random-network (CRN) model. Several approaches have been proposed for representing a

tetrahedrally coordinated CRN [4–7]. However, these theoretical models predict an amorphous phase denser than its crystalline counterpart, contrary to experimental observations (see [8] and references therein). In fact, the presence of voids in most of the deposited amorphous films is responsible for the amorphous phase density being smaller than the crystalline one. In our previous work [9], we have shown in the case of a-Si that the inclusion of nanometric voids in a CRN model accounts for the reduction of its density in comparison with the crystalline one. Moreover, this nanoporous model of a-Si gives structural and dynamical properties in better agreement with experiment than the CRN ones [9, 10]. Experimental measurements [11, 12] show that the voids are also present in amorphous silicon–carbon alloys. Following these observations, our nanoporous structural model of a-Si has been extended to simulate the structure of the Si-rich a-$Si_{1-x}C_x$ system: one has only to replace, with probability x, silicon atoms by carbon ones.

The supercell approach [9] is chosen to describe the structural and the chemical disorder in a-$Si_{1-x}C_x$ alloys. Owing to the computational limitations, periodic boundary conditions have been used to avoid surface effects. In order to obtain the equilibrium atomic coordinates in the supercell, a relaxation procedure is needed to minimize the deformation energy of the system. After the minimum total strain energy is reached and the equilibrium positions of all the atoms in the supercell are obtained, the vibrational eigenstates or normal-mode frequencies are determined by diagonalization of the dynamical matrix. An approximation of the DVS is obtained by sampling the vibrational frequency spectrum. In order to obtain a smooth DVS, we have used twenty-seven wavevectors uniformly distributed in the irreducible supercell Brillouin zone [9].

As we are concerned with covalent tetrahedrally bonded solids, the short-range interatomic interactions prevail. The phenomenological model currently used to describe the short-range valence forces in these systems is the valence-force-field (VFF) model. In the present work, the strain description is based on a VFF potential given by [13]

$$V = \tfrac{1}{2}\sum_i \sum_j \tfrac{1}{2}k_r(\Delta r_{ij})^2 + \tfrac{1}{2}\sum_i \sum_j \sum_k \tfrac{1}{2}k_\theta(r_0\,\Delta\theta_{jik})^2 \qquad (1)$$

where the i-summation is taken over all the atoms in the supercell, whereas the summations over j and k are restricted to the nearest neighbours of atom i. Δr_{ij} and $\Delta\theta_{jik}$ are the variations of the distance between atoms i and j, and the angle between two adjacent bonds (i, j) and (i, k), respectively, from their equilibrium values. k_r and k_θ are the bond-stretching and the bond-bending force constants, respectively.

We used this interatomic potential model to relax the structure out of equilibrium, on the one hand, and to determine its vibrational eigenstates in its equilibrium configuration, on the other hand.

4. Results and discussion

In this section we present the results of our detailed vibrational analysis of Si-rich a-$Si_{1-x}C_x$ films. We present first the recorded Raman spectra, then the densities of vibrational states computed for structural models of a-$Si_{1-x}C_x$ systems. Finally, we show how to conveniently interpret the short-range topological and chemical disorder in these amorphous alloys by calculating the total Raman spectra.

4.1. Raman scattering in a-$Si_{1-x}C_x$ alloys

Figure 1 depicts Raman spectra for hydrogenated a-Si (a) and a-$Si_{1-x}C_x$ thin films with alloy compositions $x = 0.21$ (b) and $x = 0.43$ (c), over a wide frequency range including both

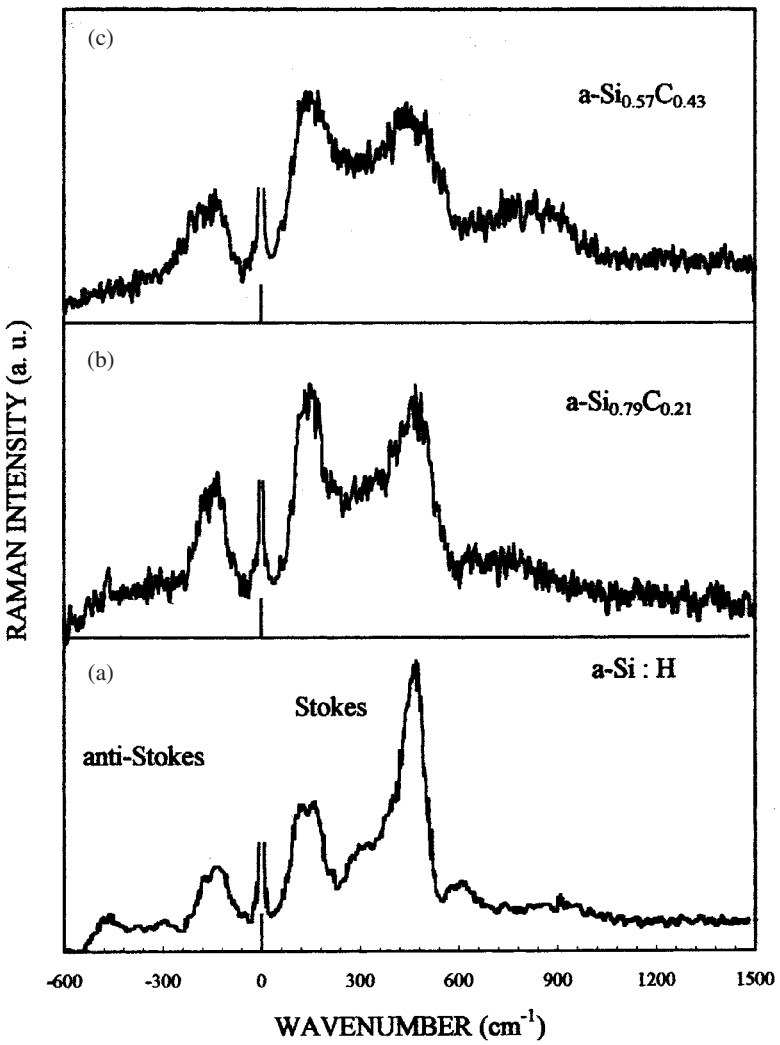

Figure 1. Experimental Stokes and anti-Stokes Raman spectra of a-Si:H (a), a-$Si_{0.79}C_{0.21}$ (b) and a-$Si_{0.57}C_{0.43}$ (c), obtained at room temperature with the 488 nm excitation line.

Stokes ($\omega > 0$) and anti-Stokes ($\omega < 0$) sides, and multiple-order processes. The Raman spectrum of a-Si:H has already been reported and investigated by Zwick and Carles [2]; it is reported here for comparison.

The three spectra show non-intense and broad bands, which are characteristic of highly disordered solids. The coherence length of the vibrational modes in these films does not exceed a few interatomic distances, and the main bands are assigned as Raman signatures of the vibrational density of states of the corresponding materials.

The Raman spectrum of a-Si:H (figure 1(a)) shows two prominent structures merging in the first-order frequency range, centred around 150 and 480 cm^{-1}. These two bands are attributed to scattering by transverse acoustic-like (TA-like) and optical-like (TO-like) modes, respectively [2]. Beyond the cut-off frequency (520 cm^{-1}), a second-order optic band centred at 980 cm^{-1} is clearly visible.

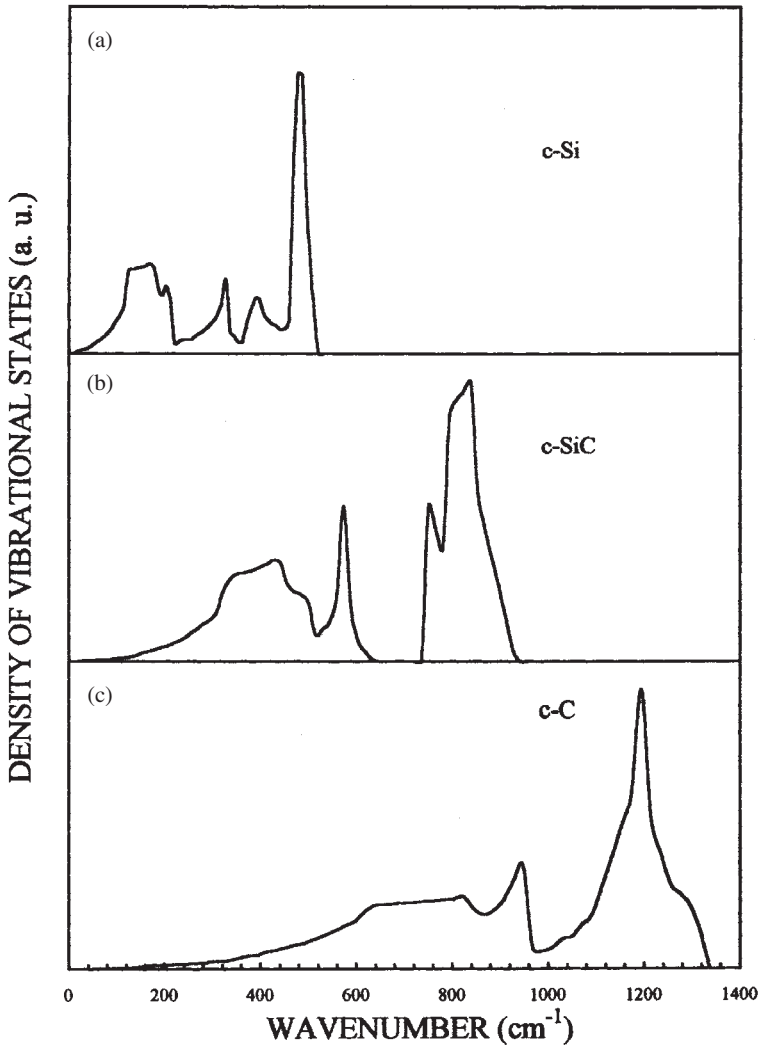

Figure 2. Calculated densities of vibrational states of crystalline materials: (a) c-Si, (b) c-SiC, and (c) diamond-like c-C. The calculation is performed using the VFF model with the force-constant values given in the text.

In Raman spectra of a-$Si_{1-x}C_x$ films (figures 1(b) and (c)), three main bands are clearly visible. An analysis based on the DVS of crystalline Si, SiC, and diamond-like C (see figure 2), shows that these three bands are easily assigned to acoustic-like modes (50–150 cm^{-1}) and Si–Si and Si–C optical-like modes (400–500 cm^{-1} and 600–900 cm^{-1}, respectively). Of particular relevance is the absence of a distinct C–C optical-like band, which is expected in the high-frequency range (>1000 cm^{-1}). The same trends have been reported previously in hydrogenated a-$Si_{1-x}C_x$ thin films with $x = 0.25$ for which a total chemical ordering was expected [1].

By comparison with the a-Si Raman spectrum (figure 1(a)), the replacement of Si atoms by C ones is seen to induce additional states between the acoustic- and optical-like bands, and beyond the cut-off frequency (520 cm^{-1}). This trend is enhanced on increasing the alloy composition variable x (figure 1(c) versus (b)).

The first-order structures are also observed on the anti-Stokes side where their intensity rapidly decreases versus frequency: this is due to Bose–Einstein population factor effects. Furthermore, a broad background is spread under all of the above-mentioned features. This structureless underlying signal has already been recognized in Raman spectra of amorphous solids and it has been shown that it arises mainly from multiple-order Raman scattering [2, 14].

4.2. Density of vibrational states of a-$Si_{1-x}C_x$ alloys

In order to check the assignments made above, the structure of a-$Si_{1-x}C_x$ alloy ($x < 0.5$) has been modelled and the corresponding DVS has been calculated numerically. As a first approximation, we have neglected the anharmonic effects [15], and we have taken for the mixed bond-bending force constant $k_\theta^{XXY} = k_\theta^{XXX}$ (X, Y = Si or C). The VFF parameters, k_r and k_θ, have been fixed at their crystalline values: they have been chosen in such a way as to reproduce in a satisfactory manner the DVS of c-Si, c-SiC, and diamond-like c-C.

The computed crystalline densities of states are displayed in figure 2, with $k_r = 131.92$ N m^{-1} and $k_\theta/k_r = 0.034$ for c-Si, $k_r = 224.25$ N m^{-1} and $k_\theta/k_r = 0.071$ for c-SiC, and $k_r = 316.55$ N m^{-1} and $k_\theta/k_r = 0.13$ for c-C. From this figure, it can be noted that our results compare favourably with those reported in the literature [16–18], except as regards some details which are not important as we are dealing with disordered phases.

The densities of states computed for structural models of a-$Si_{1-x}C_x$ alloys with $x = 0.21$ and 0.43 are displayed in figures 3 and 4, respectively: in (b) the replacement of Si atoms by C ones is random, whereas in (c) the occurrence of homonuclear C–C bonds has been computationally avoided. Hence the spectra 3(c) and 4(c) can be used as a check for the chemical ordering which is expected in Si-rich a-$Si_{1-x}C_x$ alloys [1]. For comparison, the as-recorded Raman spectra are shown at the top in these figures (only the Stokes parts are shown).

The three main bands observed in the Raman spectra are found in our simulations, keeping in mind that their relative intensity must be multiplied by their corresponding polarizability derivatives for directly comparing with the Raman cross-section. As a matter of fact, these results clearly show that the Si–C bond vibrations give a smaller contribution than the Si–Si ones to the Raman efficiency. As shown in figures 3 and 4, the DVS for a-$Si_{1-x}C_x$ models with partial chemical order (spectra (b)) displays noticeable changes in comparison with that calculated with total chemical ordering (spectra (c)). In spectra (b), we note, in particular, a redistribution of the vibrational states leading to the distortion of the acoustic band, to the disappearance of the band gap between 600 and 700 cm^{-1}, and to the appearance of vibrational modes around 1000 cm^{-1}. These trends are enhanced on increasing the carbon content (figure 4 versus figure 3). A careful observation of the spectra (a)–(c) shows that the shape of the low-frequency Raman spectrum (0–600 cm^{-1}) will be better reproduced with spectra (b) than (c). A direct comparison between spectra (a) and (b) shows that the Raman spectrum does not mirror the total DVS of the alloys. Consequently, further work is needed to calculate the Raman spectrum of a-$Si_{1-x}C_x$ alloys. Indeed, bond polarizability and multiple-order Raman scattering [2, 14] must be taken into account.

To characterize the alloy vibrations, we have calculated the projected densities of states projected on the three types of bond embedded in the amorphous alloy, as was already done by Bouchard *et al* [19] in the case of the a-$Si_{1-x}Ge_x$ system. The bond-projected DVS for bonds of type X–Y (X, Y are Si or C) was defined as [19]:

$$g^{(X-Y)}(\omega) = \sum_n \delta(\omega - \omega_n) \frac{\sum_{(i,j)}^{XY} \sum_\alpha |u_{n\alpha}^i - u_{n\alpha}^j|^2}{\sum_{(i,j)} \sum_\alpha |u_{n\alpha}^i - u_{n\alpha}^j|^2} \tag{2}$$

where $u_{n\alpha}^i$ is the displacement of the ith atom in the direction α ($=x, y, z$) from its equilibrium

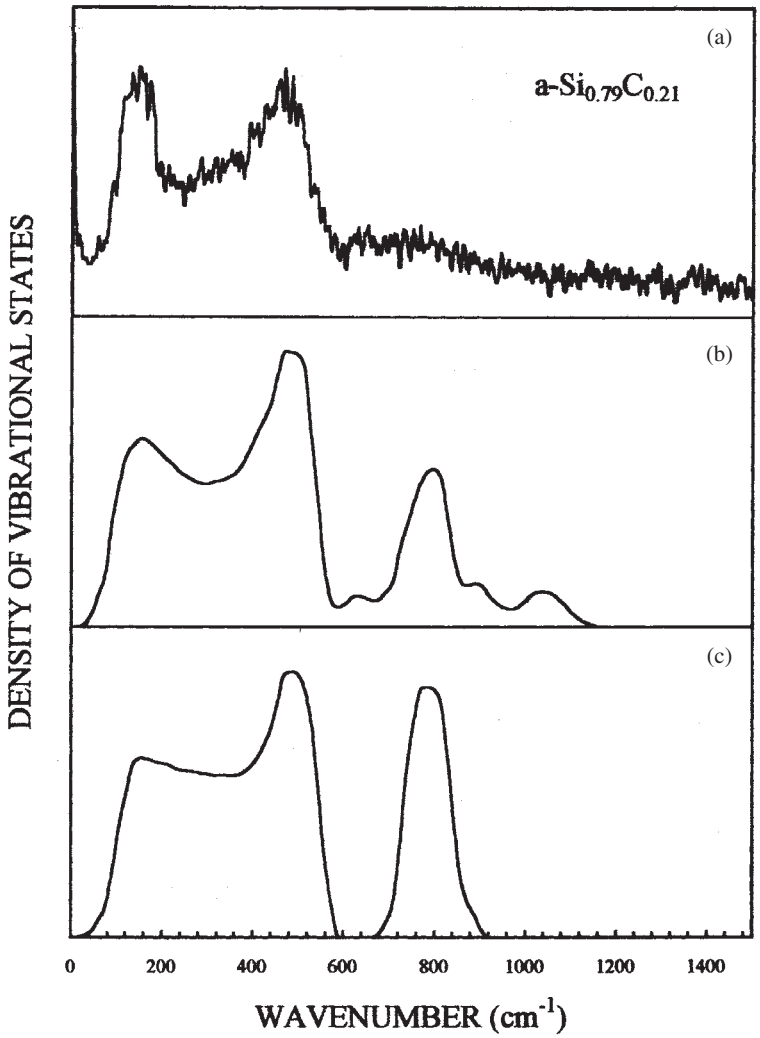

Figure 3. Comparison between the as-recorded Stokes spectrum of a-$Si_{0.79}C_{0.21}$ film (a) and the calculated DVS of the corresponding structural models without (b) and with (c) total chemical order.

position for the vibrational mode with frequency ω_n. The summation in the denominator is taken over all the nearest-neighbour atom pairs (i, j), whereas in the numerator it has been restricted to those of (X, Y) type.

The densities of vibrational states projected on the Si–Si, Si–C, and C–C bonds are displayed in figure 5. Also shown in this figure are the corresponding total DVS. As expected, the DVS projected on the Si–Si bond shows, in the spectral range 0–600 cm^{-1}, two prominent bands centred at 150 and 480 cm^{-1}. The band intensities as well as their ratio decrease on increasing the carbon content. In this spectral range, the DVS projected on the Si–C bond shows a nearly flat band, which increases in magnitude with the alloy composition variable x, leading to the disappearance of the gap between the two Si–Si bands. At higher frequencies (>600 cm^{-1}), this Si–C-projected DVS shows an intense band at 800 cm^{-1} and two less

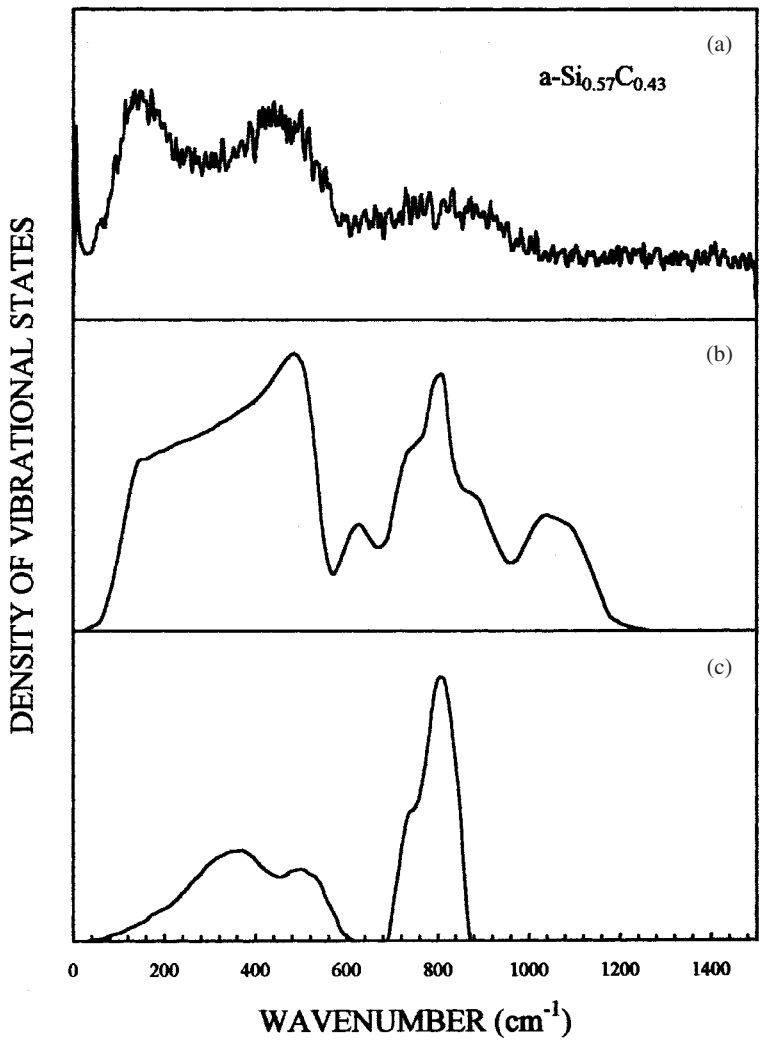

Figure 4. Comparison between the as-recorded Stokes spectrum of a-$Si_{0.79}C_{0.21}$ film (a) and the calculated DVS of the corresponding structural models without (b) and with (c) total chemical order.

intense features on both sides, i.e. at 650 and 1050 cm^{-1}. If the main features of the DVS projected on the Si–Si and Si–C bonds can be expected from the corresponding densities of states of crystalline phases, this is not the case for that projected on the C–C bond. Indeed, in the spectral range 0–600 cm^{-1}, the DVS projected on the C–C bond shows a non-intense and broad band centred at 350 cm^{-1}, whereas in this frequency range a smoothly increasing DVS is expected [1] (see also figure 2(c)). Moreover, the band of the C–C stretching modes, which is expected at about 1200 cm^{-1}, is found to lie at lower energies ($\sim$1050 cm^{-1}) for the a-$Si_{1-x}C_x$ alloy.

From the results of using this projection technique, it is now clear that the shape as well as the evolution with content x of the low-frequency Raman spectrum (0–600 cm^{-1}) of a-$Si_{1-x}C_x$ films is governed primarily by the DVS projected on the Si–Si bond. Therefore, the contribution

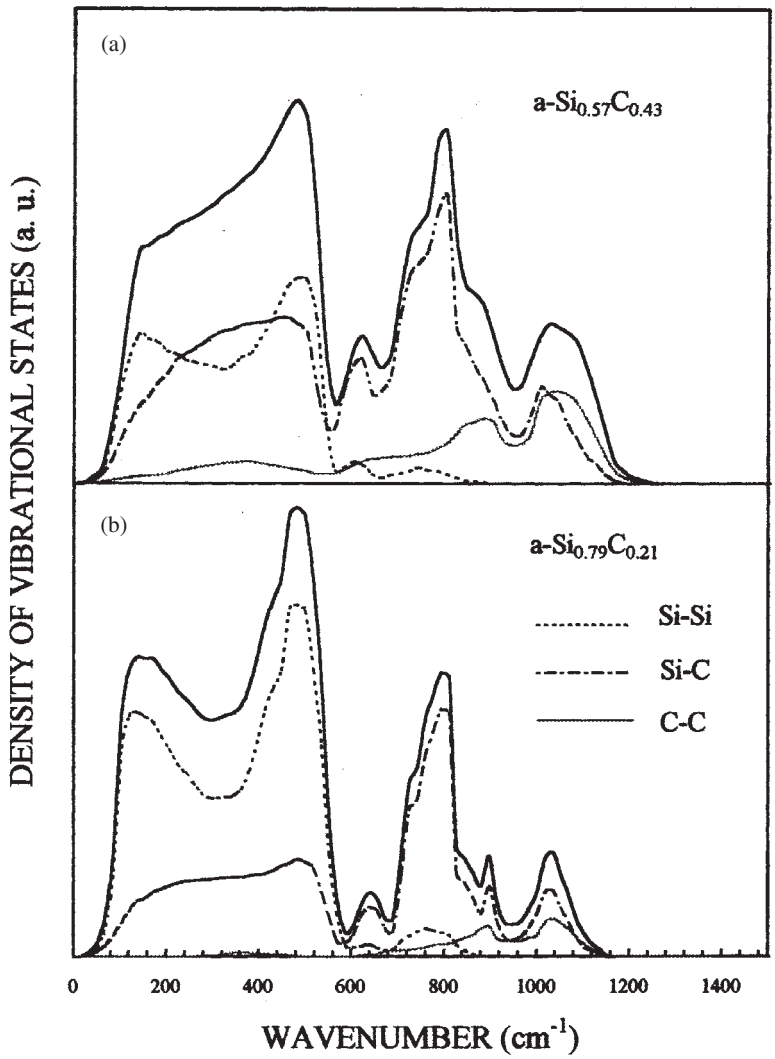

Figure 5. Bond-projected densities of states computed without total chemical order for structural models of a-$Si_{1-x}C_x$ alloys with $x = 0.21$ (a) and $x = 0.43$ (b). The solid line is the total density of states.

of the DVS projected on the Si–C bond to the Raman spectrum is thus tremendously reduced, as can also be noted at higher frequencies for the optical-like Si–C band. These facts confirm the high Raman efficiency of the Si–Si bond relative to the Si–C one. Unlike the Si–Si- and Si–C-projected densities of states, the DVS projected on the C–C bond does not give marked features in the Raman spectrum. It must give rather a structureless signal, underlying the Si–Si and Si–C bands, which increases in magnitude with increasing carbon content.

4.3. Modelling of the Raman spectra

As already mentioned, a reliable model for describing the whole shape of the Raman spectra has been achieved for a-Si [2] and a-GaAs [14]. We intend in this section to show how this

model accounts for the Raman spectrum of a-$Si_{1-x}C_x$ thin films and its evolution versus alloy composition. In the following, we briefly outline the main features of this model and then we present its results for a-$Si_{1-x}C_x$ alloys.

4.3.1. The proposed model. In highly disordered or amorphous materials, the translational invariance or long-range order disappears, and the Raman selection rules and the wavevector conservation law are no longer valid. All vibrational modes, their overtones, and their combinations (additive and subtractive) are allowed. The total Raman intensity results from the summation over these different contributions and is written as follows:

$$I = \sum_n \alpha_{n/1} I^{(n)} \tag{3}$$

where n represents the scattering order. The coefficients $\alpha_{n/1}$ account for the decrease with n of the scattering efficiency and $\alpha_{1/1}$ equals 1. If one assumes that all selectivity is effectively lost, the order-n contribution $I^{(n)}$ is given by convoluting n times the first-order one. Then one gets

$$I^{(n)} = [I^{(1)}]^{\otimes n} \tag{4}$$

where the superscript $\otimes n$ stands for the order-n autoconvolution product.

In the framework of Shuker and Gammon's model [20], the first-order Raman intensity is written as follows:

$$I^{(1)} = A\left[\frac{\tilde{n}(\omega, T) + 1}{\omega}\right] C(\omega) g(\omega). \tag{5}$$

Here A accounts for the optical properties of the sample, $g(\omega)$ is the DVS of the amorphous material, $C(\omega)$ is the coupling coefficient for the light and the vibrational modes, and $\tilde{n}$ is the Bose–Einstein population factor. On defining $g(-\omega) = g(\omega)$ and $C(-\omega) = C(\omega)$, and keeping in mind that the respective population factors obey the following relation:

$$\frac{\tilde{n}(\omega, T) + 1}{\omega} = \frac{\tilde{n}(-\omega, T)}{(-\omega)} \tag{6}$$

equation (5) describes well the first-order Raman scattering for both Stokes ($\omega > 0$) and anti-Stokes ($\omega < 0$) processes. Therefore, equations (4) and (5) account for the whole spectrum, Stokes and anti-Stokes parts, and all the processes (additive and subtractive, combinations, and overtones) with their appropriate population factors.

The construction of the Raman spectra of amorphous materials requires the knowledge of the density of states, $g(\omega)$, the coupling coefficient $C(\omega)$, and the scaling factors $\alpha_{n/1}$. These latter can be estimated from the measured integrated intensities of crystal Raman spectra, and the former can be determined directly from numerical modelling. The frequency dependence of the coupling coefficient $C(\omega)$ is given by a phenomenological model as follows [2]:

$$C(\omega) = |\omega|\left[1 - \exp\left(-\frac{|\omega|}{\omega_0}\right)\right] \tag{7}$$

where absolute values are used to maintain $C(-\omega) = C(\omega)$. The peculiar frequency ω_0 is expected to be the Debye limit, which is located in the crystal just below the low frequency of the zone-edge acoustic mode, i.e. the TA(L) phonon in diamond-like crystals [16].

4.3.2. The results for a-$Si_{1-x}C_x$ alloys. The contribution of each type of bond to the total first-order Raman scattering in a-$Si_{1-x}C_x$ film was evaluated first, according to relation (5), using the DVS projected on the Si–Si, Si–C, and C–C bonds shown in figure 5. The frequency dependence of the coupling coefficient is given by equation (7), in which the frequency ω_0

is fixed at 110 cm^{-1} corresponding to the TA(L) phonon in c-Si. The total first-order Raman spectrum is derived then from a weighted sum of the preceding individual contributions. The adjustment of the weighting factors is carried out using the total Raman spectra (see the following). The final fitted values are 1, 0.2, and 0.1 for the Si–Si, Si–C, and C–C contributions, respectively. The multiple-order (up to eight) Raman spectra were deduced next, from the first-order spectrum, according to the relation (4). Finally, taking $\alpha_{2/1} = 0.4$ and $\alpha_{n/1} = 0.17$ for $n = 3$–8 [2] in the relation (3), the calculation of the total Raman spectrum has been achieved.

The calculated Raman spectra at room temperature for a-$Si_{1-x}C_x$ alloys with $x = 0$, 0.21, and 0.43 are displayed (as continuous lines) in figure 6. In the same figure, the corresponding experimental spectra are reproduced as dots.

A good agreement between experiment and calculation is observed for a-Si as well as for Si-rich silicon–carbon alloys. Not only do the Stokes and anti-Stokes first-order structures fit, but also the broad background scattering is well reproduced throughout the spectral range explored. However, small discrepancies are observed in the shapes of the Si–Si and Si–C optical-like bands. These might be due to the approximations made in our theoretical treatments. In particular, the anharmonic effects and the Coulomb interactions have been neglected. The same trends are expected with the more recently proposed empirical interatomic potential of Tersoff [21], at least for the Si–C optical-like bands, because of the short range of this potential (any explicit ionic behaviour is omitted in the present potential).

The comparison between theory and experiment argues in favour of a highly disordered phase, in which the carbon atoms are randomly distributed on the sites of a tetrahedrally coordinated amorphous silicon network. Therefore, total chemical ordering in amorphous silicon–carbon alloys is not achieved, even at low carbon substitution rates, in contrast to our previous expectation [1].

5. Conclusion

Raman spectroscopy is a versatile tool for analysing dynamical properties and short-range order in amorphous solids. It is particularly efficient if one treats all of the data, on the one hand, and if one couples this characterization technique with numerical modelling, on the other hand.

In this paper, a detailed vibrational analysis of chemically deposited Si-rich a-$Si_{1-x}C_x$ thin films has been reported. Raman scattering has been measured over a wide range of frequencies. In order to interpret the Raman response, the structure of the a-$Si_{1-x}C_x$ system ($x < 0.5$) has been modelled and the corresponding vibrational eigenstates have been computed in the harmonic approximation. By calculating the DVS projected on the Si–Si, Si–C, and C–C bonds, and taking into account the difference between the Raman activities of these bonds, a fit of the empirical Raman spectra has been achieved, by integrating Stokes and anti-Stokes, first-order, and multiple-order processes.

In contrast to the case for C-deficient sputtered a-SiC films [22], there is no clustering of carbon atoms in our chemically deposited Si-rich a-SiC thin films according to our analysis. But this does not exclude the possibility of the occurrence of homonuclear carbon bonds in these samples; C–C bonds are found to be highly dispersed in a tetrahedrally coordinated a-Si network.

From our previous [1] and the present analyses, we can conclude that the short-range chemical order in a-$Si_{1-x}C_x$ alloys is partial, since C–C and Si–Si bonds occur in Si-rich and C-rich films respectively. The case of the a-$Si_{1-x}C_x$ system with $x \geqslant 0.5$, in which hybridization disorder of C atoms is expected, merits analysis via Raman spectroscopy and numerical modelling, as done here for the relatively simple case of Si-rich alloys. This will provide valuable help in achieving a better understanding of the microstructure of such complex systems.

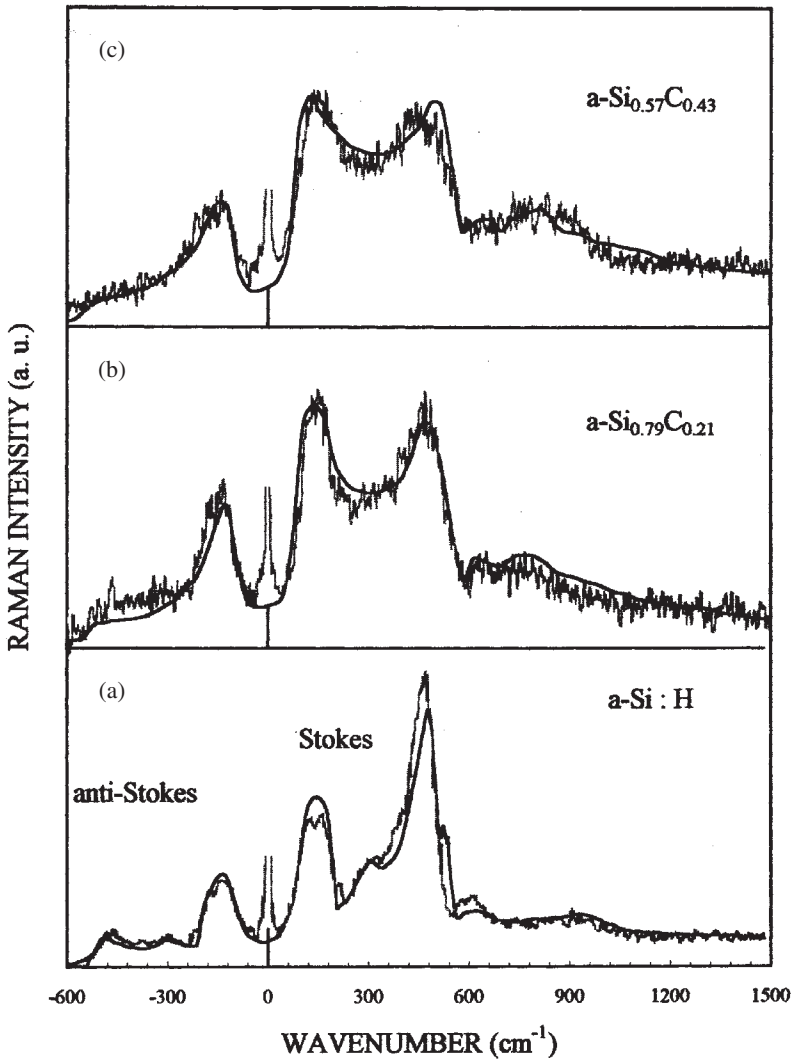

Figure 6. Comparison between the experimental (dots) and theoretical (continuous lines) Raman spectra of a-$Si_{1-x}C_x$ alloys with $x = 0$ (a), $x = 0.21$ (b), and $x = 0.43$ (c). The calculation is performed using the DVS computed for structural models of a-Si (after [9]) and a-$Si_{1-x}C_x$ alloys with partial chemical ordering (see figure 5).

Acknowledgment

The authors are indebted to Dr Silvey Schamm of the CEMES Laboratory of Toulouse in France for the amorphous silicon–carbon samples used in this study.

References

[1] Chehaidar A, Carles R, Zwick A, Meunier C, Cross B and Durand J 1994 *J. Non-Cryst. Solids* **169** 37
[2] Zwick A and Carles R 1993 *Phys. Rev.* B **48** 6024
[3] Schamm S, Kihn Y, Sevely J, Lespiaux D and Langlais F 1992 *Proc. 10th European Congr. on Electron*

Microscopy (Granada, Spain, Sept. 1992) vol 1, ed A Rios, J M Arias, L Megras-Megras and A Lopez-Galindo p 277
[4] Duffy M G, Boudreaux D S and Polk D E 1974 *J. Non-Cryst. Solids* **15** 435
[5] Alben R, Weaire D, Smith J E Jr and Brodsky M H 1975 *Phys. Rev.* B **11** 2271
[6] Etherington G, Wright A C, Wenzel J T, Dore J C, Clarke J H and Sinclair R N 1982 *J. Non-Cryst. Solids* **48** 265
[7] Wooten F and Weaire D 1987 *Solid State Physics* vol 40 (New York: Academic) p 1164
[8] Kuster J S, Thompson M O, Jacobson D C, Poate J M, Roorda S, Sinke W C and Paepen F S 1994 *Appl. Phys. Lett.* **64** 437
[9] Chehaidar A, Djafari Rouhani M and Zwick A 1995 *J. Non-Cryst. Solids* **32** 405
[10] Chehaidar A 1995 *PhD Thesis* No 1987, Paul-Sabatier University, France
[11] Mousseau N and Thorpe M F 1993 *Phys. Rev.* B **48** 5172
[12] Carreno M N, Pareyra J, Fantini M C and Landers R 1994 *J. Appl. Phys.* **75** 538
[13] Martinez E and Cardona M 1983 *Phys. Rev.* B **28** 880
[14] Chehaidar A, Zwick A, Carles R and Bandet J 1994 *Phys. Rev.* B **50** 5345
[15] Dietrich B, Osten H J, Rucker H, Methfessel M and Zaumseil P 1994 *Phys. Rev.* B **49** 17 185
[16] Weber W 1977 *Phys. Rev.* B **15** 4789
[17] Windl W, Pavone P, Karch K, Schut O, Strauch D, Giannozzi P and Baroni S 1993 *Phys. Rev.* B **48** 3164
[18] Windl W, Karch K, Pavone P, Schut O, Strauch D, Weber W H, Hass K C and Rimai L 1994 *Phys. Rev.* B **49** 8764
[19] Bouchard A M, Biswas R, Kamitakahara W A, Grest G S and Soukoulis C M 1988 *Phys. Rev.* B **38** 10 499
[20] Shuker R and Gammon R W 1970 *Phys. Rev. Lett.* **26** 642
[21] Tersoff J 1989 *Phys. Rev.* B **39** 5566
[22] Gorman M and Solin S A 1974 *Solid State Commun.* **15** 761